Contents lists available at ScienceDirect

Biochimica et Biophysica Acta

Review

Proteorhodopsin[☆,☆☆]

Christian Bamann [a,*], Ernst Bamberg [a], Josef Wachtveitl [b], Clemens Glaubitz [c]

[a] Max Planck Institute of Biophysics, Max-von-Laue Straße 3, 60438 Frankfurt am Main, Germany
[b] Johann Wolfgang Goethe University, Institute for Physical and Theoretical Chemistry, Max-von-Laue Straße 7, 60438 Frankfurt am Main, Germany
[c] Johann Wolfgang Goethe University, Institute for Biophysical Chemistry & Centre for Biomolecular Magnetic Resonance, Max-von-Laue Straße 9, 60438 Frankfurt am Main, Germany

ARTICLE INFO

ABSTRACT

Proteorhodopsins are the most abundant retinal based photoreceptors and their phototrophic function might be relevant in marine ecosystems. Here, we describe their remarkable molecular properties with a special focus on the green absorbing variant. Its distinct features include a high pK_a value of the primary proton acceptor stabilized through an interaction with a conserved histidine, a long-range interaction between the cytoplasmic EF loop and the chromophore entailing a particular mode of color tuning and a variable proton pumping vectoriality with complex voltage-dependence. The proteorhodopsin family represents a profound example for structure–function relationships. Especially the development of a biophysical understanding of green proteorhodopsin is an excellent example for the unique opportunities offered by a combined approach of advanced spectroscopic and electrophysiological methods. This article is part of a Special Issue entitled: Retinal Proteins—You can teach an old dog new tricks.

© 2013 Elsevier B.V. All rights reserved.

1. Introduction

The recent attention attracted by the rhodopsin family is certainly driven by the new field of optogenetics that is becoming a standard technique in neurobiological sciences [1–3]. The light-driven ion transport is exploited for changing the membrane potential and thereby for triggering downstream events. While this is an "old trick for new dogs", rhodopsins are still a dynamic field of research. In the past it was mainly bacteriorhodopsin (bR) catalyzing the application of advanced and novel spectroscopic techniques to biomolecules. Recent findings in the last fifteen years expanded both the spectrum of functions and the distribution of rhodopsins. The latter finding led to the surprising conclusion that rhodopsins are found in all phyla of life [4–6] and it might be the most abundant phototrophic system on this planet [7]. With the new rhodopsins came the observation that they represent a rather versatile family of proteins while retaining the structural scaffold of seven transmembrane helices (TMHs) with a retinal chromophore bound to a conserved lysine. By

far the most abundant family members belong to the proteorhodopsins (pRs) that are the focus of this review. They act as proton pumps with a high similarity to bR [4], but showing different properties that make them a case study for the structure function relationship of a membrane protein. New features worth the effort of investigation are especially (1) color tuning, (2) long range conformational coupling, (3) a His-Asp cluster working as a proton dyad and (4) the pH-dependency of proton transport vectoriality.

Proteorhodopsin has also been a model case for the concerted application of advanced biophysical methods, which unfold their full potential if applied in a synergistic manner (Fig. 1). Hence, this review focuses rather on recent achievements in the understanding of the molecular properties of pRs, than on describing all the fascinating aspects of new rhodopsins, that is the evolution of retinylidene photoreceptors and their biological function or the contribution of retinal based photosynthesis to energy fixation. A short overview about the initial identification and description of the prototypic green proteorhodopsin (GPR) is presented but the reader is referred to relevant reviews [8–10] and related contributions in this special issue for further details. Here, we will give a brief overview about the historical background and the ecological impact of pRs with only selected references.

2. Phylogenetic background and in vivo function

The discovery of the first pR (GPR) came as a surprise as it presented the first evidence of a bacterial retinal-based photoreceptor [4]. GPR was not isolated from its native host, but was identified in a metagenomic screening of uncultured sea samples from the Monterey Bay in California. Such a strategy provides essential information
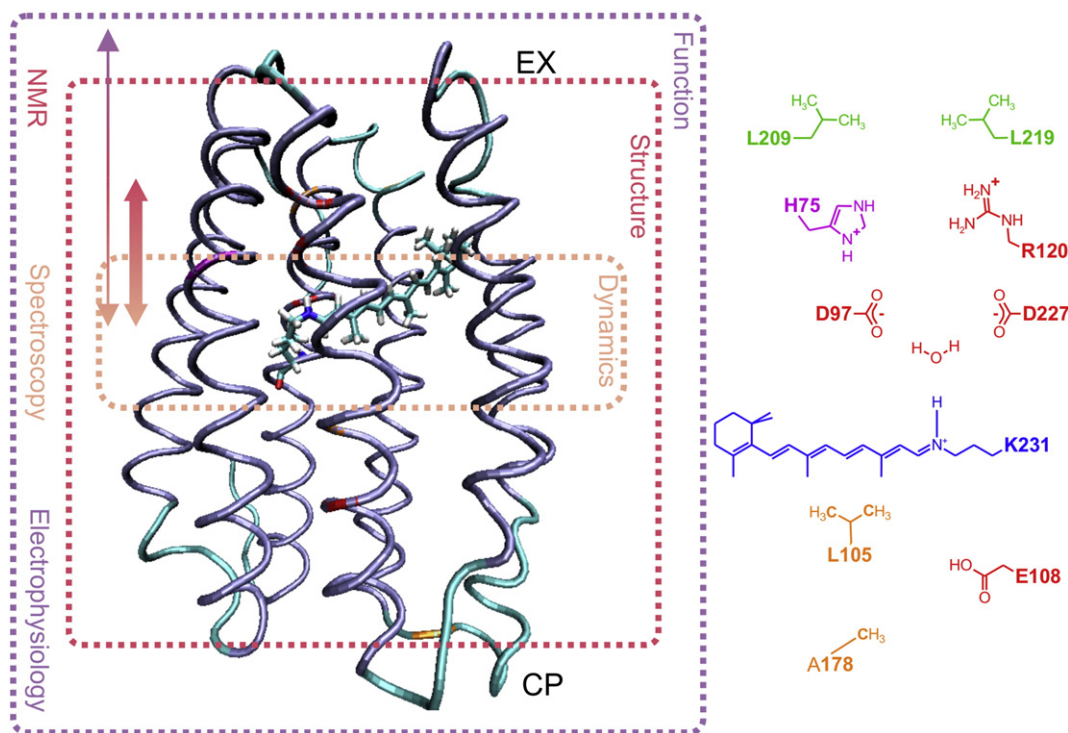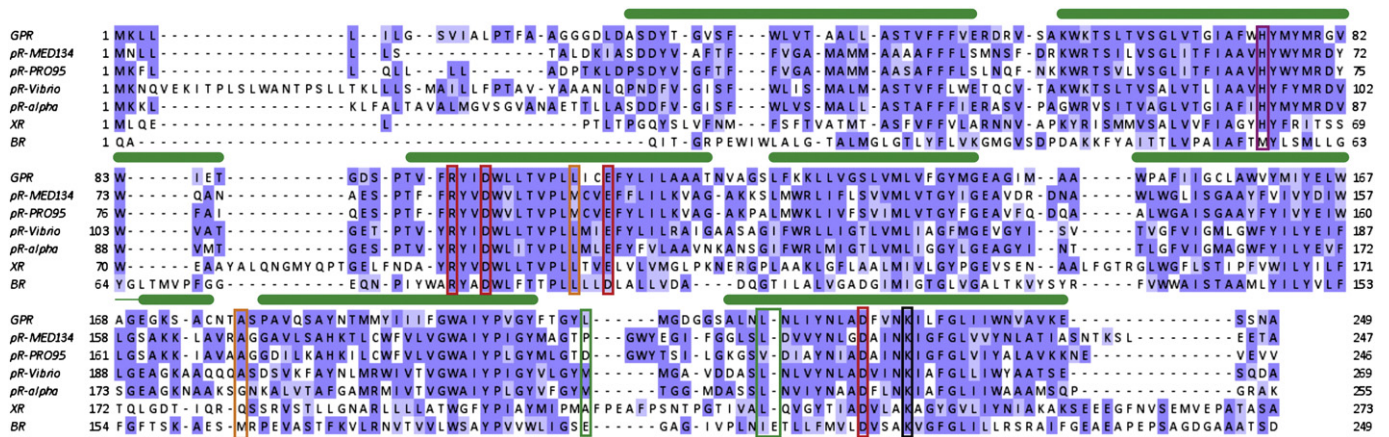
Fig. 1. Structural model of GPR based on PDB ID: 2l6x [57] and rationale for the experimental workflow. TMHs and loop regions are shown in blue and green cartoon representation, respectively. The relevant residues are color-coded as in Fig. 2: the conserved histidine in pRs (magenta), counter-ion complex and proton donor (red), color tuning residues L105 and A178 (orange), residues found at the position where the proton release group (PRG) would be expected (green).

about microbial communities and allows the collection and comparison of a wealth of data from different geographic areas [11]. Further identification in more marine microbial populations supported the high prevalence of pRs and it made retinal-based phototrophy a widespread oceanic phenomenon [12]. The name proteorhodopsin refers to the initial identification in the group of γ-proteobacteria (SAR86). Since then, hundreds of pR-like sequences alone have been monitored in the Sargasso Sea [13]. They are not confined to a single taxon or a single location as they appear to be distributed in many microorganisms from all over the world [14–19]. In fact, pR-like genes have been further monitored in freshwater habitats [20–22], in sea ice [23], on high mountains [24] or even in Siberian permafrost samples [25]. The host organisms are as diverse as well and they cover viruses [26], many different classes of bacteria, archaea [27,28] and eukaryotic marine protists [9,29–31]. Lateral gene transfer confers a high genetic mobility of pR genes among the bacterioplankton and supports their wide distribution and abundance [27]. So the proteorhodopsins really deserve their name from the Greek god Proteus who had the ability to change his physical appearance.

Most marine species' were collected from the photic zone where light and its perception is an important quality affecting the life cycle of the organism. Interestingly, the natural biological function of pRs has not been described definitely in most cases and it may vary among the different species' [32]. Like bR, the pRs described so far can work as proton pumps and this property could be linked to a purely phototrophic function. The ability of light energy fixation was transferred genetically to a host system where the *in vivo* effect of pR activity manifested itself in physiological functions like flagellar motility or ATP synthesis [33,34]. There are reports about light-stimulated growth that was related to the presence of a pR for example in the flavobacterium *Dokdonia* sp. MED134 (Fig. 2, [35]), concluding that the expression of pR imparts fitness to the host under stress condition like starvation. However, this is not the general case as is shown for a closely related strain from *Dokdonia* sp. PRO98 [36]. Recently, there has been a profound demonstration of the later quality in a bacterium from *Vibrio* sp. that

is amenable to genetic manipulation. Light-induced survival fitness under starvation conditions could be clearly correlated to the transcription of pR (Fig. 2, [37]). Therefore, more attempts will lead to the transition to cultured samples allowing a more rigorous control of the growth conditions [19,36,38,39]. In addition there is a single report about a photosensoric function of a pR in the heterotrophic protist *Oxyrrhis marina* [31]. This notion is challenged by the finding of pR expression in an endomembrane system linked to a phototrophic function [30]. Proton pumping could be demonstrated in vitro [40] for one of the rhodopsins from *O. marina*. Both results are interesting as they add a new context, either phototaxis or organelle energizing, to the photoreceptor's function which can be addressed in further studies.

Two other properties of pRs are noteworthy as signs of pRs' physiological importance or as a form of molecular adaptation. Spectral tuning of pR is exploited to optimize light absorption at different depths in the sea. Blue light absorbing variants, blue proteorhodopsin (BPR), have a higher prevalence in deeper areas of the photic zone where blue light can still penetrate, while other parts of the visible spectrum are already filtered [12]. On the molecular level such an adaptation is mainly determined by a single amino acid substitution at position 105 in GPR (Fig. 2, see below) [41]. The second property relates to another variation of the rhodopsin theme. Here, a rhodopsin forms a stable entity with an additional chromophore factor building up the smallest antenna complex in photoreceptors. Such a structure was first observed in a rhodopsin, xanthorhodopsin, from the eubacterium *Salinibacter ruber* that binds an additional carotenoid, salinixanthin [42]. Energy transfer from the S_2 state of salinixanthin to the retinal chromophore enlarges the spectral sensitivity of this photoreceptor [43,44]. The tight binding of the additional chromophore to the protein was outlined in the crystal structure of the xanthorhodopsin [45]. The close distance and the rigidness are prerequisites for an efficient energy transfer. The presence of small antenna complexes also seems to be further spread among bacterioplankton [36]. Until now there has been one other documentation in a pR from *Gloeobacter violaceus* that could also be successfully reconstituted with

```
GPR        1  MKLL--------L--ILG--SVIALPTFA-AGGGDLDASDYT-GVSF---WLVT-AALL-ASTVFFFVERDRV-SAKWKTSLTVSGLVTGIAFWHYMYMRGV  82
pR-MED134  1  MNLL--------L-LS---------TALDKIASDDYV-AFTF---FVGA-MAMM-AAAAFFFLSMNSF-DRKWRTSILVSGLITFIAAVHYWYMRDY        72
pR-PRO95   1  MKFL--------L-QLL--LL-----ADPTKLDPSDYV-GFTF---FVGA-MAMM-AASAFFFLSLNQF-NKKWRTSVLVSGLITFIAAVHYWYMRDY       75
pR-Vibrio  1  MKNQVEKITPLSLWANTPSLLTKLLLS-MAILLFPTAV-YAAANLQPNDFV-GISF---WLIS-MALM-ASTVFFLWETQCV-TAKWKTSLTVSALVTLIAAVHYFYMRDV  102
pR-alpha   1  MKKL--------KLFALTAVALMGVSGVANAETTLLASDDFV-GISF---WLVS-MALL-ASTAFFFIERASV-PAGWRVSITVAGLTGIAFIHYMYMRDV   87
XR         1  MLQE--------L--------PTLTPGQVSLVFINDA-ASFVFYVARNNV-APKYRISMMVSAVVFIAGYHYFRITSS                           69
BR         1  QA----------------QIT-GRPEWIWLALG-TALMGLGTLYFLVKGMGVSDPDAKKFYAITTLVPAIAFTMYLSMLLG                         63

GPR        83 W-----IET---------GDS-PTV-FRYIDWLLTVPLLICEFYLILAAATNVAGSLFKKLLVGSLVMLVFGYMGEAGIM--AA----WPAFIIGCLAWVYMIYELW   167
pR-MED134  73 W-----QAN---------AES-PTF-FRYVDWVLTVPLMCVEFFLILKVAG-AKKSLMWRLIFLSVVMLVTGYIGEAVDR-DNA----WLWGLISGAAYFVIVYDIW   157
pR-PRO95   76 W-----FAI---------QES-PTF-FRYVDWLLTVPLLCVEFYLILKVAG-AKPALMWKLIVFSVIMLVTGYFGEAVFQ-DQA----ALWGAISGAAYFVIVYEIW   160
pR-Vibrio  103 W-----VAT--------GET-PTV-YRYIDWLLTVPLLICEFYLILRAIGAASAGIFWRLLIGTLVMLIAGFMGEVGYI--SV----TVGFVIGMLGWFYILYEIF   187
pR-alpha   88 W-----VMT--------GES-PTV-YRYIDWLITVPLLMLEFYFVLAAVNKANSGIFWRLMIGTLVMLIGGYLGEAGYI--NT----TLGFVIGMAGWFYILYEVF   172
XR         70 W------EAAYALQNGMYQPTGELFNDA-YRYVDWLLTVPLLTVELVLMGLPKNERGLAAKLGFLAALMIVLGYPGEVSEN-AALFGTRGLWGFLSTIPFVWILYILF   171
BR         64 YGLTMVPFGG----------EQN-PIYWARYADWLFTTPLLLDLALLVDA----DQGTILALVGADGIMIGTGLVGALTKVYSYR-----FVWWAISTAAMLYILYVLF   153

GPR        168 AGEGKS-ACNTASPAVQSAYNTMMYIIIFGWAIYPVGYFTGYL--------MGDGGSALNL-NLIYNLADFVNKILFGLIIWNVAVKE---------SSNA  249
pR-MED134  158 LGSAKK-LAVRAGGAVLSAHKTLCWFVLVGWAIYPIGYMAGTP---GWYEGI-FGGLSL-DVVYNLGDAINKIGFGLVVYNLATIASNTKSL------EETA   247
pR-PRO95   161 LGSAKK-IAVAAGGDILKAHKILCWFVLVGWAIYPLGYMLGTD---GWYTSI-LGKGSV-DIAYNIADAINKIGFGLVIYALAVKKNE--------VEVV   246
pR-Vibrio  188 LGEAGKAAQQQASDSVKFAYNLMRWIVTVGWAIYPLGYMLGV----MGA-VDDASL-NLVYNLADVINKIAFGLLIWYAATSE---------SQDA   269
pR-alpha   173 SGEAGKNAAKSGNKALVTAFGAMRMIVTVGWAIYPLGYVFGYV----TGG-MDASSL-NVIYNAADFLNKIAFGLIIWAAAMSQP----------GRAK  255
XR         172 TQLGDT-IQR-QSSRVSTLLGNARLLLLATWGFYPIAYMIPMAFPEAFPSNTPGTIVAL-QVGYTIADVLAKAGYGVLIYNIAKAKSEEEGFNVSEMVEPATASA  273
BR         154 FGFTSK-AES-MRPEVASTFKVLRNVTVVLWSAYPVVWLIGSE-----GAG-IVPLNIETLLFMVLDVSAKVGFGLILLRSRAIFGEAEAPEPSAGDGAAATSD  249
```

Fig. 2. Sequence alignment of different pRs and bR. GPR—green pR from the γ-proteobacterium SAR68; pR-MED134—pR from *Dokdonia* sp. MED134 showing light-stimulated growth; pR-PRO95—*Dokdonia* sp. PRO95 showing no light-stimulated growth; pR-Vibrio—pR from *Vibrio* sp. used for genetic targeting; pR-alpha—pR from the α-proteobacterium SAR11 (*Peligobacter* sp.); XR—xanthorhodopsin from *Salinibacter ruber*; bR—bR from *Halobacter salinarum*. The alignment is color coded by the BLOSUM62 matrix. TMHs are indicated by green bars according to the NMR data for GPR [54,57]. Relevant functional residues are marked by boxes and include the conserved histidine (magenta), residues involved in proton transfer and in complex counter-ion formation (red), color tuning (orange) and those found instead of the PRG in bR (green). The lysine residue forming the pSB with the retinal is indicated in the black box. Details are found in the text and Fig. 1.

carotenoids [46,47]. As suggested for xanthorhodopsin and confirmed in the experiments with the pR from *Gloeobacter violaceus*, the important factors for the antenna binding is the 4-keto ring in the carotenoid chromophore and the presence of a small glycine residue (G156 in xanthorhodopsin) that gives enough space for the 4-keto ring in the protein binding groove.

3. Molecular determinants of pRs and the structural building blocks

So far, we have addressed the classification of pRs from a phylogenetic point of view as abundant retinal-based photoreceptors found mainly in marine protists. There are additional molecular markers that allow for a further classification of these photoreceptors. Compared to the archaeal proton pumps with the prototypic bR, there are several pronounced differences to GPR, the prototype of the pR class: First the aforementioned spectral tuning factors in GPR and BPR (Figs. 1 & 2, L105), second the presence of a histidine in TMH B (H75), and third the absence of the bR-typical proton release group (PRG) including two glutamic acids [48,49]. GPR undergoes a bR-like photocycle (Fig. 5D) characterized by different intermediates usually termed K (product of photoisomerization), M (deprotonated Schiff-base, [SB]), N (re-protonated Schiff-base, [pSB]) and O (or PR', late intermediate). The spectral intermediates and their kinetics are sensitive indicators for structural and protonation changes (see below). As for their geographical and taxonomic distribution, we find also differences for the molecular markers among the different pRs. Most of the studies published so far were concerned with the prototype GPR. Spectroscopic and structural studies will be added from other pRs where it is relevant.

3.1. Structural studies on GPR—the benefits from NMR spectroscopy

Green proteorhodopsin has been extensively studied by solid-state NMR. This technique offers unique possibilities for a structure and dynamics characterization as well as for mechanistic studies once the pentameric/hexameric GPR complexes (see below) are reconstituted into lipid bilayers. Solid-state NMR on ^{13}C-labeled retinal incorporated into GPR revealed an almost 100% all-*trans* population in the ground state (Fig. 3, [50]) in agreement with Raman data [51], whereas a minor content of 13-*cis* retinal was detected in retinal extraction experiments [52]. The use of dynamic nuclear polarization (DNP) to enhance the sensitivity of solid-state NMR enabled the probing of small conformational changes within the retinal chromophore upon introducing color changing mutations (Fig. 3, [53]).

Based on an extensive chemical shift assignment, a detailed secondary structure and dynamics analysis was carried out revealing the structural scaffold of GPR and confirming the predicted seven TMH fold [54,55]. The retinal chromophore is bound to the opsin via a protonated Schiff-base formed with Lysine K231. The characteristic kinks that have been observed in other rhodopsins [56] are also conserved in GPR, including the proline kink at P201 in TMH F and the π-bulge in TMH G starting at position N230. Main structural differences are mainly confined to the loops connecting the TMHs. Noteworthy are the small B–C loop located at G87 to P90 forming a β-turn, and the E–F loop that bears a helical extension from E170 to N176. There is a good agreement between solid-state and liquid-sate NMR data (see below) on GPR in
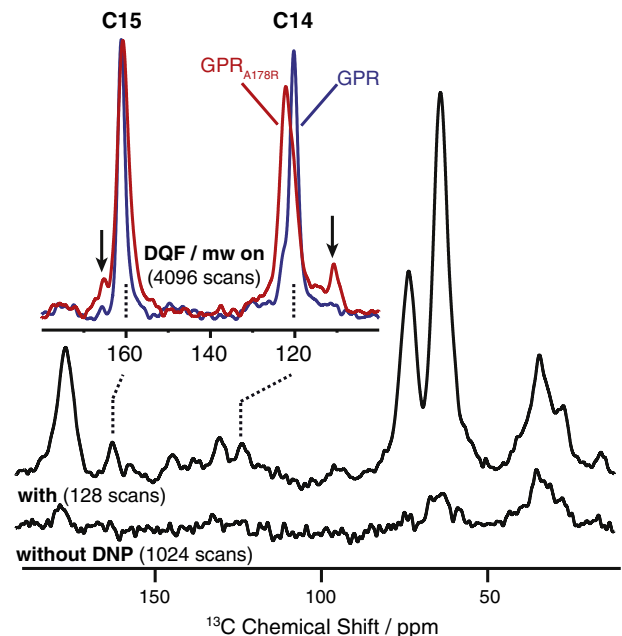
Fig. 3. DNP-enhanced ^{13}C-MAS NMR spectra of 14–15-^{13}C-labeled retinal in GPR and GPR$_{A178R}$ [53]. The use of DNP enables a significant signal enhancement as shown for the comparison between a conventional spectrum and a DNP enhanced cross polarization spectrum (bottom). The C14 and C15 resonances are extracted by applying a double quantum filter experiment (DQF, top). Upon introducing a mutation in the distant EF loop (A178R), chemical shift changes for C14 and a small population of 13-*cis* retinal (arrows) are observed.
Figure adapted from [53].

liposomes and micelles, respectively [54,57]. Additional experimental evidence for mobility of the A–B, C–D, and F–G loops has been presented, the latter potentially being linked to the GPR ion transporting function [55]. It was also shown that the molecular dynamics of especially helices C, F and G but also the EF loop are coupled to the dynamic bilayer properties as they show increasing mobility when switching from the gel phase to the liquid crystalline phase [58]. Solid-state NMR data have also revealed the formation of a specific interaction between H75 and D97 (see below) [59] and provided an understanding of the role of the EF loop for color tuning (see below) [53].

GPR proved to be an excellent test case for the applicability of cell-free expression of membrane proteins and their suitability for structure analysis. Using a *tour-de-force* liquid-state NMR approach on GPR in diC7PC micelles, in which it assumes a monomeric form, its 3D backbone structure has been determined [57] (Fig. 1) and its dynamics has been analyzed [60]. The seven TMHs A to G arrange in a similar manner as in other rhodopsins (e.g. [56], Fig. 1). This study shows that de novo 3D structures of a cell free produced membrane protein can be obtained and functional data showed that the activity of cell free produced GPR is not compromised [57].

Further insights into the molecular details are derived from the xanthorhodopsin structure [45] and several properties were also detected in GPR. The close environment of the protonated Schiff-base is dominated by the complex counter-ion that is formed in GPR by the residues D97, D227 and R94 (Fig. 1). At alkaline pH, a water molecule is in a complex with the two charged aspartic acids and the proton from the protonated Schiff-base to which it is strongly hydrogen-bonded [52]. The R94 shows only a weak coupling to D97 [61] and is in line with a side chain orientation pointing away from D97 as in the xanthorhodopsin structure. Instead, an important and pR specific interaction is observed between D97, the primary proton acceptor in the pump cycle, and H75 located in TMH B. An eminent feature of GPR is the high pK_a-value of the proton acceptor D97 (~7.5) that is among other factors the result of its interaction with H75 (see below).

3.2. Oligomeric state

In lipid bilayers, green proteorhodopsin forms donut-shaped complexes with a diameter of about 40 Å as observed by cryo-electron microscopy on 2D crystalline preparations [62]. Atomic force microscopy revealed that these complexes are formed by hexamers and pentamers [63] and such complexes are even found in DDM (0.08–1%) detergent micelles [64,65]. Site-directed spin labeling and EPR in combination with Overhauser DNP have been used to construct a model for the GPR subunit arrangement within these hexameric complexes [65] (Fig. 4). In this model, GPR shows a radial arrangement with residue 177 in the EF loop pointing away from the hexamer and residue 55 in the BC loop facing the hexamer interior. In contrast, monomers are found in diC7PC micelles [57]. Within the membrane, these complexes are formed under many different conditions indicating that the hexamer/pentamer represents the native state of GPR.

In detergent, GPR is active in both monomeric and oligomeric preparations as judged from its photodynamics. However, quantitative differences exist, especially regarding the lifetime and the absolute population of the M-state varying from one to several tens of milliseconds. While this dependence on environmental factors might be not surprising, conclusions have to be seen within this context. For example fast proton release with the rise of the M-state has been observed in DHPC micelles [66], whereas this process is retarded to the end of the photocycle in detergent treated membranes from *E. coli* [51]. Likewise changes are seen in the multiplicity of the C=N vibration, a marker for the pSB environment, when going from the detergent octyl-glucoside (doublet) to lipid reconstituted samples (singlet) [67]. Whether these arise from differences in the oligomeric state or from the different detergent environment cannot be decided at this point.
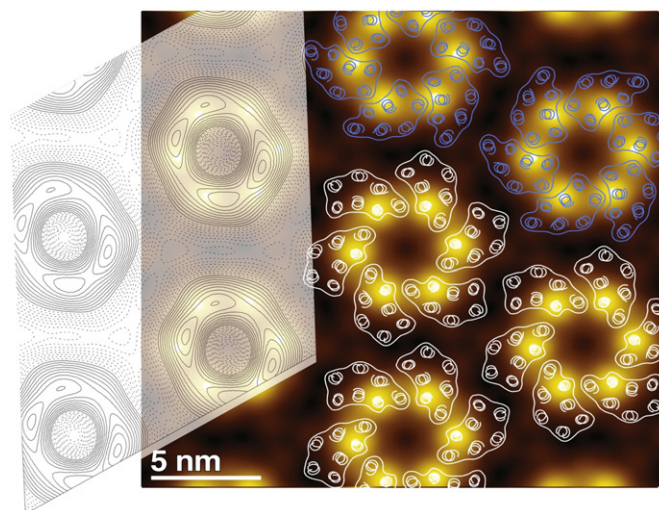
Fig. 4. Oligomeric form of GPR in lipid bilayers. A low-resolution cryo-EM projection map in negative stain [62] revealing a ring-shaped assembly. It was shown by AFM image analysis of crystalline and non-crystalline sample preparations, that these rings are mainly formed by GPR hexamers [63]. A radial arrangement of GPR within the hexamers has been shown by EPR spectroscopy [65].

Similar effects have also been described for a pR from *O. marina* [40] and a pR from *Exiguobacterium sibiricum* [68]. In the latter case the titration of the proton acceptor and the M-state kinetics are shifted by ~2 pK units in a lipidic environment. Besides of environmental conditions, also specific molecular factors influencing the oligomeric state have been reported. For example, it was found for the pR from *Gloeobacter violaceus* in detergent micelles that trimer formation is linked to pH-dependent interactions between the conserved histidine in TMH B (H75 in GPR) and the primary proton acceptor [69]. A similar study has not been reported yet for GPR. However, GPR has been found to form monomers or lower oligomers in a nanodisk structure, which shows that external factors can shift the oligomerization equilibrium [70,71]. Such a strategy could serve as a benchmark to further probe the influence of environmental factors on GPR's or other pR's activity.

One could speculate whether the radial arrangement of PR within these complexes offers an advantage for light harvesting in the sea and results in a better quantum yield per pumped proton compared to monomers. Experimental evidence to support such a hypothesis is still lacking.

### 3.3. Molecular mechanisms of color tuning

Proteorhodopsin comprises two main families, a green absorbing one (GPR, $\lambda_{max.} = 525$ nm) found closer to the surface and a blue absorbing one (BPR, $\lambda_{max.} = 490$ nm) found at greater depths [41]. It is generally accepted that the spectral characteristics of the retinylidene chromophore is strongly affected by its interaction with amino acids located in its direct vicinity. For example, one single point mutation GPR_{L105Q} in GPR, which is close to the chromophore, shifts the absorption maximum towards blue, while the corresponding BPR_{Q105L} mutation in BPR causes a green shift [41,72]. The nature of position 105 could affect the environment around the C13-methyl group and might also influence the hydrogen-bonding strength of the pSB proton with the surrounding water molecules [67].

The recent discovery of a 20 nm red shift of the GPR absorption spectrum upon a single mutation GPR_{A178R} in the EF loop came therefore as a great surprise as the mutation site is far away from the retinylidene [73]. This effect is highly position specific [74]. A similar long-range effect, induced by a mutation in the BC-loop, has only been reported for halorhodopsin [75]. Based on their data, Kandori and co-workers suggested that having a small residue such as alanine at position 178

is essential to blue shift the absorption of GPR at neutral pH into a color range compatible with a marine environment [76].

The molecular basis for this EF-loop induced color shift has recently been resolved by solid-state NMR supported by dynamic nuclear polarization and time-resolved optical spectroscopy [53]. By comparing ^{13}C- and ^{15}N chemical shifts between wild type GPR and GPR_{A178R}, mutation-induced structural changes throughout the protein have been mapped. Interestingly, these changes propagate from the EF loop along helices E and F throughout the whole protein including the retinal binding pocket (Fig. 5A–C). A direct effect on the retinal structure was observed by ^{13}C chemical shift changes within the retinal itself at positions C14 and C15 at the end of the polyene chain. The primary reaction was probed by pump-probe spectroscopy, which revealed that the formation of the K-like photointermediate is almost pH-independent and slower compared to the wild type, while the decay of the K-intermediate is accelerated, suggesting structural changes within the counterion complex upon mutation. The whole photocycle in the μs–s time range was monitored by flash photolysis experiments (Fig. 5E), which were analyzed using a reaction scheme proposed earlier [77]. An additional photointermediate was necessary to satisfactorily simulate the experimental data attributed to an interconversion of several N-intermediates (termed N_1 and N_2). Fig. 5D shows an overview of the photocycle dynamics of GPR and GPR_{A178R}. The decay of the K-intermediate and the formation of the M-intermediate are dramatically accelerated for GPR_{A178R}. In contrast to this the later steps of the photocycle, mainly the lifetimes of the N_1, N_2 and O intermediates are prolonged. This leads to an overall photocycle duration that is 10-fold longer for GPR_{A178R} compared to GPR. The distorted EF loop structure
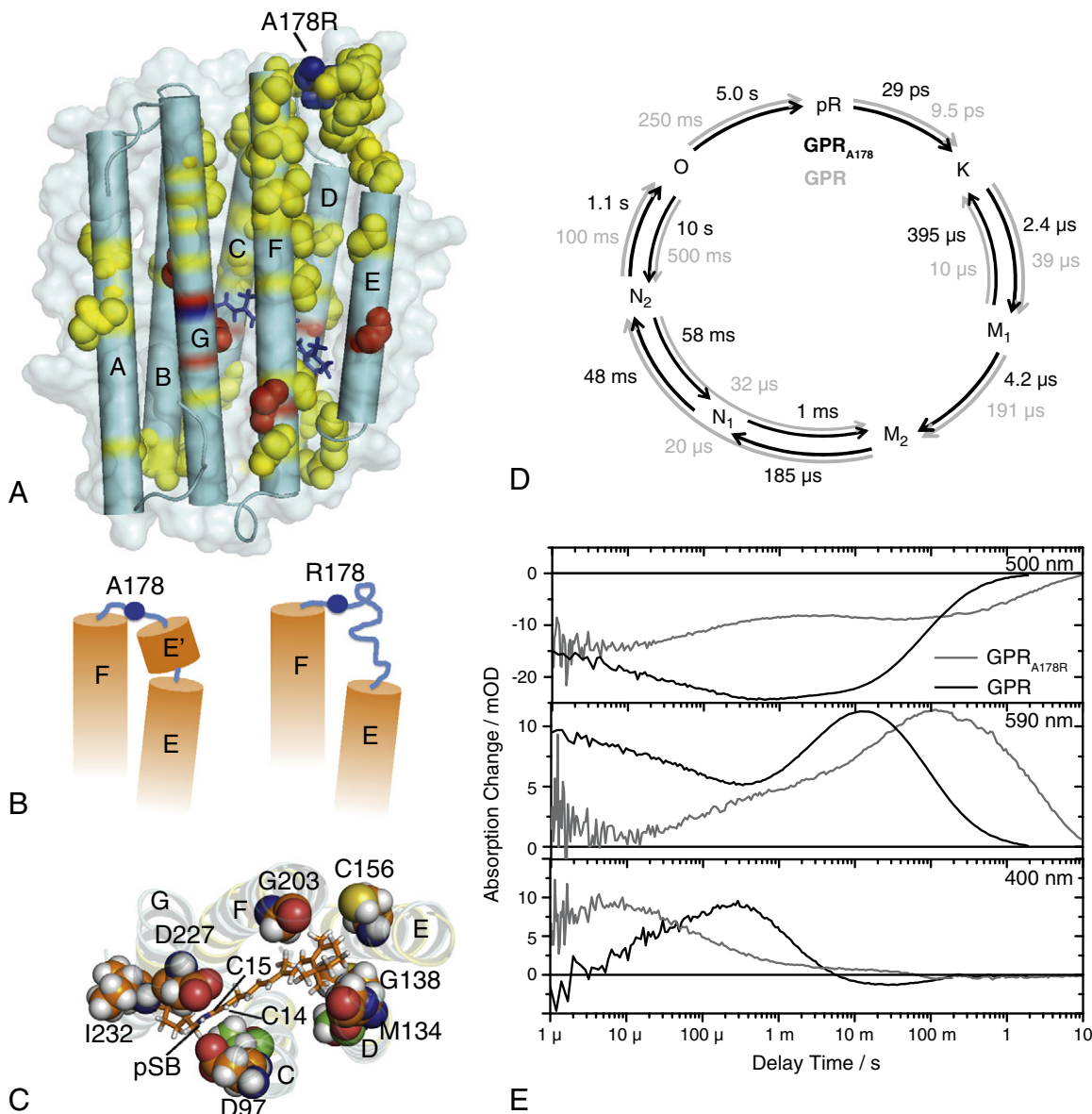
Fig. 5. Replacing A178 in the EF loop with a more bulky residue such as R causes significant structural changes in GPR resulting, in a red shift and altered photodynamics. Residues for which mutation-induced chemical shift changes are observed by solid-state NMR are highlighted in the backbone structure from Fig. 1(A). An interaction pathway from the EF loop to the retinal binding pocket can be envisaged. The observed chemical shift changes indicate that the secondary structure in the EF loop is distorted (B). A number of residues are directly located within or close to the retinal binding pocket including the primary proton acceptor D97 and D227. Chemical shift changes within these residues indicate slight structural rearrangements, which can explain the altered optical and kinetic properties (D). The reaction schemes (D) were calculated from laser-flash induced transient absorption changes (E). Laser-flash induced transient absorption changes were detected at pH 9 for GPR_{A178R} and GPR. The transients are representative for the dynamics of the ground state population (500 nm), the K-decay at early delay times and the formation of the N/O-intermediates at late delay times (590 nm) and the formation and decay of the M-intermediate (400 nm). Data show in particular a slow-down of the last steps of the photocycle, which are associated with a reorientation of helices E and F.
Figure adapted from [53].

in GPR$_{A178R}$ probably results in weaker structural constraints of the EF loop onto helices E and F with consequences for the photocycle steps involving movements of these helices. The EF loop structures could restrain helix movements during the photocycle, which become more relaxed in the mutant. For GPR, photocycles between 100 and 200 ms have been reported [51,52,70,78]. The longer photocycle for GPR$_{A178R}$ is caused by the elongated lifetime of the N/O intermediate and the interconversion of two different N intermediates. The decay of these intermediates is correlated with the reprotonation of the primary proton donor. It has been observed in bR that this step of proton uptake involves an outward motion of helix F that facilitates the proton uptake from the cytoplasmic side, most probably due to the entrance of water molecules [79–82]. After proton uptake from the cytoplasmic surface this outward movement of the F-helix is reversed [83]. Assuming a similar mechanism in GPR leads to the conclusion that the restoring force imposed by the structured EF loop to helices E and F is significantly reduced in GPR$_{A178R}$ resulting in slower helix reorientation and an elongated lifetime of the N/O intermediate. Therefore, the native EF loop seems to play a major role in proton uptake from the cytoplasmic side of GPR. This conclusion is also supported by a combined EPR and DNP study in which altered hydration levels upon illumination indicated an EF loop movement [84]. The data also show that an interaction pathway exists between EF loop and retinal binding pocket. One could speculate that signals could be transmitted across the membrane needed for potentially additional functions of GPR, such as sensing or signaling.

3.4. His-Asp cluster

GPR contains a highly conserved histidine at position 75. Homology modeling predicts its location in helix B close to the active site and near the primary proton acceptor D97 (Fig. 1) [85].

Using site-directed mutagenesis and time-resolved Fourier-transformed infrared (FTIR) spectroscopy, a direct interaction between H75 and D97 and a direct involvement in proton transfer has been suggested [86]. A possible direct interaction between both residues but no effect on the pSB was also reported [87]. Direct evidence for the formation of a pH-dependent H-bond between H75 and the primary proton acceptor D97 was provided by solid-state NMR, explaining the unusually high pK$_a$ of D97 (Fig. 6) [59] in accordance with theoretical studies on model compounds [88].

The functional role of H75 has been further studied using site directed mutagenesis in combination with black lipid membrane (BLM) experiments and time-resolved optical spectroscopy. Ultrafast vis-pump/vis-probe experiments on GPR$_{H75N}$ showed that the primary reaction dynamics are retained (Fig. 6A), while flash photolysis experiments revealed an accelerated photocycle. Despite its stabilizing function, His75 apparently slows down the photocycle in wildtype GPR and is not essential for proton transfer. The existence of a similar His-Asp cluster has been shown in xanthorhodopsin [45] and in pRs from *Gloeobacter violaceus* (see above) [69], from *O. marina* [40] and from *E. sibiricum* [68].

From the phenotype of different H75 mutants, it was concluded that the His-Asp cluster is not the only effector on the pK$_a$ of D97. In the pR from *O. marina*, no interaction was found at neutral pH and the proton acceptor has a low pK$_a$ value. For the pR from the *E. sibiricum*, a similar low pK$_a$ value was found and it was concluded from the photodynamics that the His-Asp cluster keeps the proton acceptor deprotonated during the photocycle [68] enabling proton pumping under acidic conditions. Hence, this conserved interaction for the pR-family comes in different variations and a general mechanism does not prevail at the present stage.

4. Photocycle and proton pumping

There is now profound knowledge about the light-induced isomerization of the chromophore that we summarize in the next section. The following steps are characterized by different intermediates with the main conclusion that protonation reactions at the Schiff-base lead to a
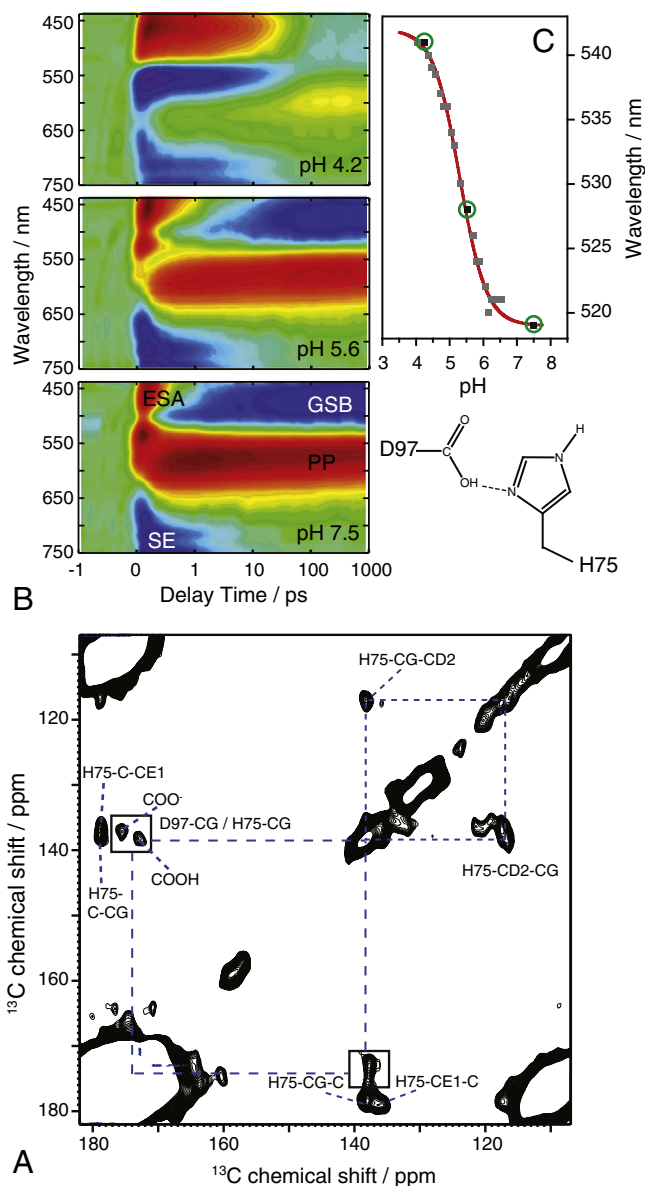
Fig. 6. The role of His75 in GPR. (A) The close proximity of His75 and Asp97 was found by ^{13}C–^{13}C correlation spectroscopy, while the nature of the H-bond formation between both side chains was revealed by ^{15}N-MAS NMR explaining the high pK$_a$ of D97 [59]. (B) Contour plots of transient absorption change of GPR$_{H75N}$ at pH 7.5, 5.6 and 4.2. The main contributions stem from excited state absorption (ESA), ground state bleach (GSB), formation of the photoproduct (PP) and stimulated emission (SE). The measurements provide a clear example that the isomerization rate is electrostatically controlled, since it is evident that the rate of the primary reaction is not determined by the pH value itself, but by the protonation state of D97 as it follows the titration curve of H75N. This leads to the effect that due to the lowered pK$_a$ of D97 in the H75N mutant, the formation of the photoproduct is still fast and efficient at pH 5.6, in contrast to GPR$_{WT}$. (C) Titration curve of GPR$_{H75N}$.

proton transfer across the membrane [4] in a bR-like photocycle. There are differences though, and especially the high pK$_a$-value of D97 leads to a composition of initial states that are different in their protonation even at physiological pH. As those are also functionally different in their pumping ability, the photocycles of the alkaline form GPR^{alk} (D97$^-$) and the acidic form GPR^{acid} (D97-H) have been investigated in great detail.
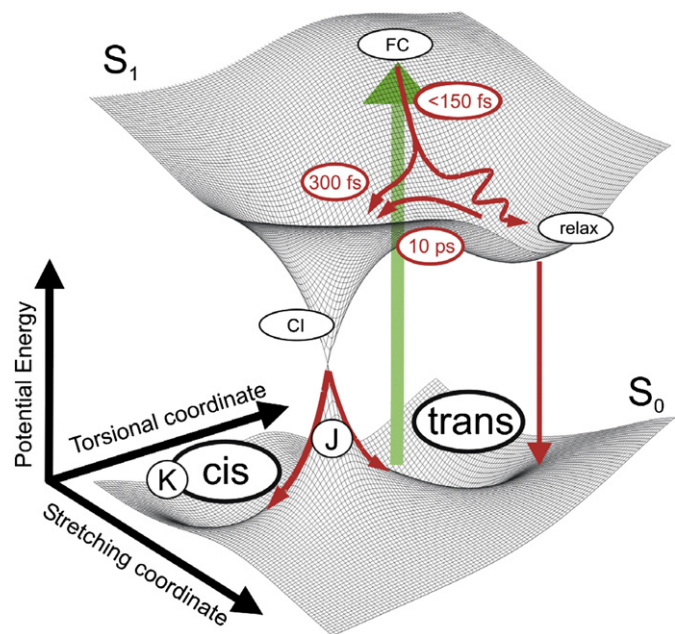
4.1. Photoisomerization

Femtosecond-time-resolved measurements on GPR in the visible [89,90] and in the IR spectral range [91] reveal the primary photoreaction

that is the general S_1 deactivation pathway up to the formation of the first ground state intermediate (K-state). Upon light excitation the ultrafast isomerization of the retinal from the all-*trans* to the 13-*cis* conformation is induced, which triggers a sequence of protein conformational changes including several proton transfer reactions. Based on the models for bR, a branched reaction scheme for the primary reaction dynamics of GPR was proposed [90]. The C=C stretching is supposed to be the first reaction coordinate out of the Franck–Condon region before the torsion around the C_{13}–C_{14} bond takes place leading to a conical intersection (CI) with the ground state. The observed biexponential decay of the excited state was explained by the assumption that some molecules do not directly reach the CI and end up in a local minimum on the S_1 potential energy surface, which has to be overcome first (Fig. 7). Particularly, it could be shown that the deactivation of the excited state possesses a pronounced pH-dependence explained by a pH-dependent tilting of the S_1 potential energy surface [90]. However, femtosecond IR spectroscopy showed that the quantum efficiency of the primary photointermediate, the K-state, is not affected by the pH/pD value [91]. The photocycle of GPR with a specifically altered proton acceptor complex was studied in H75, D97 and D227 mutants [59,92–94] and demonstrated that the negative charge of the complex counter ion is one of the main determinants of the H-bonding pattern in the retinal binding pocket and an important catalyst for the primary reaction.

4.2. Late steps in the photocycle

Several independent studies on the photocycle of GPR came to similar results and conclusions [4,51,52,60,77]. Starting from GPR[alk], the K-intermediate decays in the early microseconds range to form the M-state with a deprotonated Schiff-base. Reprotonation yields a red-shifted intermediate that returns to the initial state within tens of

Fig. 7. Reaction model for the initial photoinduced events in GPR. After photoexcitation into the Franck–Condon region (FC) two nuclear coordinates mainly contribute to the retinal isomerization. A nuclear stretch on the order of 150 fs is followed by a torsional motion on the order of 300 fs and leads to a conical intersection (CI) with the ground state. Although most molecules decay along this pathway, some will not reach the CI directly, but end up in a state on the S_1 potential energy surface separated from the CI by an energetic barrier. They can access the CI within some picoseconds and explain the biexponential decay of the excited state. The reaction proceeds on the S_0 potential energy surface (J) either back to an all-trans configuration or to the 13-*cis* state (K). This model provides an easy and straightforward interpretation of the pH-dependence of the primary reaction, since the protonation of the primary proton acceptor can be visualized in a tilting of the S_1 surface leading to different amounts of molecules ending up in the faster or slower decay channel. Figure is from [90].

milliseconds. Except for the K-state, all the kinetic intermediates from a global analysis are a mixture of the different species as a result of quasiequilibria (Fig. 5D). The M-state shows a multiphasic rise and decay whereas the early phase (~10 μs) is much faster than in bR. This is in accordance with a missing accumulation of the L-intermediate and a faster onset of structural changes that has been assigned to changes in helical segments [95]. The proton acceptor (D97) and the proton donor (E108) could be identified in mutant IR spectra. The E108 is protonated in the initial state even at pH 9 and in a stronger hydrogen-bonded network than in bR [51,52]. The second half of the photocycle is dominated by the N/O-species. IR data map it to the deprotonated E108 [52] with a 13-*cis* retinal (N-like) that decays into an O-like intermediate with a twisted all-*trans* and a protonated E108 [51,52]. In the last step deprotonation of D97 and restoration of the initial state takes place.

The M-state does not accumulate to a large extent and is dependent on the environmental conditions (see above). The maximum amplitude follows in detergent the titration curve of D97. In GPR the M-intermediate is not observed at ambient temperatures and at acidic pH when D97 is protonated. However, the M-state can be freeze-trapped (see below). That aside, there are not many differences in the photocycles of GPR[alk] and GPR[acid]. The intermediates are similar in their spectral properties [78] although no protonation changes are observed for E108 or D97 [52]. However, proton transfer reactions also take place under acidic pH.

4.3. Proton pumping and electrophysiology

4.3.1. Electrophysiological techniques in rhodopsin research

Proton pumping can be assessed either by pH-sensitive electrodes, by chromophoric pH-indicators or by measuring the charge transport associated with the proton transfer from one side to the other of the membrane. The correlation of spectroscopic markers with the signal from pH-indicators allows the determination of the kinetics for proton uptake, membrane dwell time and proton release. Furthermore, it is a comprehensive route to the stoichiometry of proton transfer per molecule and photocycle (reviewed in [96]). Complementary to the indicator approach are electrical methods. Hence in addition to proton uptake and release, any electrogenic step can be detected, for example intramolecular proton transfer reactions or proteinous charge movement connected to conformational changes. Either of those reactions will eventually give rise to the voltage dependence of the photocycle.

There are several electrical methods established and applied in rhodopsin research that all have their benefits (Fig. 8A). In principle, to detect a current from proton transfer, the proton pumps have to be oriented in an asymmetric manner with respect to the electrodes [97] in the external circuit like in (1) capacitive coupled sandwich systems [98–100], (2) in a gel matrix encapsulating pumps oriented in an electrical field [101] or (3) in cell suspensions where molecules are excited in a topographically dependent manner by a light gradient [102–104]. While the encapsulation approach (2) allows the concomitant recording of spectroscopic and electrical signals, the suspension method (3) guarantees orientation within the membrane and a native environment. The sandwich system allows the recording of stationary transport currents by increasing the conductance with ionophores. However, all the methods bear an intrinsic frequency dependence of the signal, that is, the passive properties of the electrical circuit can lead to a distortion of the signal amplitude and limit the accessible frequency window for the measurement by filtering, shunting or passive discharge [105]. Slow signals will be more affected than fast ones that are usually limited by the access resistance or the bandwidth of the electronic devices. Hence, one has to keep in mind that the different techniques can give rise to different quantitative results especially if the equivalent circuit of the system is not well defined as is often the case for experimental reasons. Furthermore, the mentioned approaches lack the control and measurement of the transmembrane voltage. While for the *in vitro* systems one can assume the absence of a voltage in the beginning of an experiment, such a condition might not be found in the case of the cell suspension (3) as *E. coli* cells
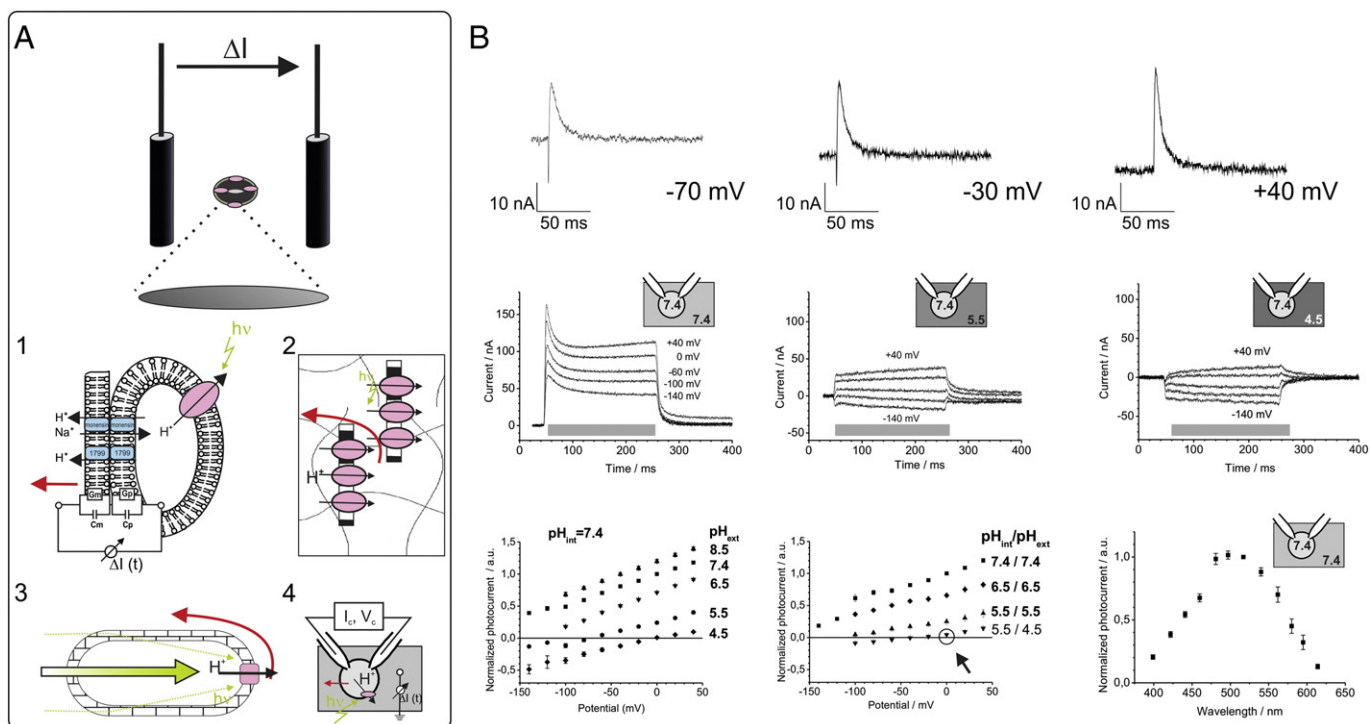
Fig. 8. GPR electrophysiology. (A) Overview of the discussed electrophysiological techniques, when a displacement current due to proton pumping of GPR (pink ellipses) between two electrodes are recorded (top). A close-up for the different approaches is shown numbered according to the text: 1) Proteoliposomes adhere to a black lipid membrane and currents are recorded by capacitive coupling. Ionophores (blue boxes) allow the measurements of (DC) transport currents [52]. 2) GPR in *E. coli* membrane fragments are oriented in an electric field and encapsulated in acrylamide gels [77,78]. 3) In the light gradient method, a lens effect by the *E. coli* cell leads to a higher probability to excite remote GPR molecules [103]. 4) Two-electrode voltage-clamp (TEVC) in Xenopus oocytes allows voltage control over the membrane. The electrodes themselves are asymmetrically distributed with respect to GPR (inside and outside of the oocyte). Two electrodes are used to record and to control the current I_c and the voltage V_c [52,115]. The red arrows should indicate the passive discharge of the systems that limits the time window of the measurements. (B) Summary of TEVC recordings. Green laser flash-induced current recorded on an oocyte expressing GPR at pH_{ext} 7.4 at different holding potentials (top panel). Stationary currents are recorded under green light illumination with varying pH_{ext} (middle panel). A summary of the current–voltage relationships and action spectrum (bottom panel).
Part (B) is modified from Lörinczi et al. [115] with permission.

can have transmembrane voltages of ~− 150 mV (e.g. [106]). Control over this parameter is achieved in voltage-clamp recordings with microelectrodes as has been shown first for bR expressed in oocytes from *Xenopus laevis* [107] and later for other rhodopsins [108,109]. One has to stress that information about the photocycle's voltage dependence cannot be gathered in any other way.

4.3.2. Transient proton and charge movements

The proton pumping ability of GPR[alk] at high pH (D97[−]) is linked to the photocycle in a similar manner as with bR [4]. The proton reactions at the Schiff-base lead to the release towards the extracellular side and the recruitment of a proton from the cytoplasmic side. After proton transfer to D97, the SB is reprotonated by E108 during M-decay. No proton release was detected upon this state. Such a behavior is similar to bR under alkaline conditions or with mutations in the PRG [49,110]. The proton uptake to E108 is linked to the rise of the N-like intermediate and proton release is followed only in the last step. Such a sequence of events has been indeed observed with pH-indicators [51] and in other pRs like the ones from *Gloeobacter violaceus* [111] or from *E. sibiricum* [68]. However, a different result was observed at alkaline pH (9.5) and in a lipid environment where a fast proton release occurs [66]. Proton release would be associated with the built-up of the M-state due to the coupling of the PRG with D97. Indeed, the M-state formation is associated with charge transfer [103], but this fact can also be related to the proton transfer from the Schiff-base to D97 alone. In the late stage of the photocycle the PRG is replenished by reprotonation from D97 [112]. The implication is mechanistically relevant as it would require involvement of another group with different protonation states in the proton transfer. It was reported that H75 undergoes protonation changes during

the photocycle [86], but mutants of GPR[H75X] are fully functional as proton pumps so that this residue cannot be a necessary factor for proton pumping [59,86]. It is interesting to note that the presence of a PRG in the absence of E194 and E204 homologues was also concluded in Channelrhodopsin-2 [113,114]. Hence, there are variations in the PRG theme that might be also found in pRs.

At acidic pH, transient charge movements could be followed after flash excitation of GPR[acid] in reconstituted systems [52,78] and in *Xenopus* oocytes under voltage-clamp conditions [115] (Fig. 8B). The direction of the transfer is inverted leading to an inward current similar to bR with a protonated H^+-acceptor D85 [116]. Interestingly, the inward current in GPR is strongly pH and voltage dependent, so that an inward current can be observed even at pH 7.5 under hyperpolarizing potentials. The participating groups in the protein are not identified yet and infrared data do not reveal fast protonation changes in the carboxylic region [52]. The transport measurements under voltage-clamp conditions point to an experimental gap between the spectroscopic and electrical measurements. However, the advent of oriented systems in a supported bilayer could help to follow the voltage-dependence of the photocycle spectroscopically [117,118]. In the sensory rhodopsin II from *Natromonas pharaonis* NPSRII, the proton transfer can be halted at the M-state by applying an electric field opposite to the proton current. Interestingly, there do not seem to be additional structural changes involved compared to the state in the absence of an applied electrical field. Therefore, it could be possible to decouple the proton reactions from the structural changes as is also clearly documented in the NpSRII[D75N] mutant (homologue to D97 in GPR) that undergoes normal movement of TMH F without built-up of the M-state [119]. Similar experiments have not been done yet for GPR or other proton pumps nor do we know if GPR undergoes similar

structural changes at acidic pH. The important observation is related to the modulation of the photocycle by an electrical field that can shunt the proton transport. This is described in detail for bR where one observes the accumulation of an M-state in a voltage-dependent manner [120]. Eventually a fraction of the molecules are trapped in a futile, non-transporting circle where reprotonation of the SB occurs from the extra-cellular side. The conclusion is supported by double illumination experiments that can specifically probe the presence of the M-state [121]. The shunting in an M-state can explain the linear current–voltage characteristics with higher currents under depolarizing conditions. Similar experiments have been also successfully performed for GPR (Fig. 8B) [52,115].

For a stationary inward transport in GPR, it would further be required that the proton from the pSB can escape to the cytoplasmic side via a cytoplasmic half channel. It was seen in the xanthorhodopsin structure that the proton donor is in a more hydrophilic environment than in bR [45]. A more important role could be due to a water molecule that is hydrogen-bonded to both the retinal binding lysine (K231 in GPR) and the proton donor (E108). E108 is more strongly hydrogen-bonded than the corresponding D96 in bR. Therefore, one could speculate that conformational changes, especially from the EF loop, under acidic conditions still proceed and lower the pK_a of E108 while keeping D97 protonated. Therefore, the high pK_a of D97 could render inward proton transport feasible (see below), especially under hyperpolarizing conditions that should speed up proton transfer towards the cytoplasmic side. As seen in Fig. 8B, inward currents can therefore be triggered at neutral pH in a voltage-dependent manner.

4.3.3. Stationary transport measurements

A qualitatively different approach to assess proton transport comes from stationary transport measurements. There is consensus about the proton transport function of GPR that is linked to an M-state [4,52,122] at alkaline pH due to the very high pK_a of D97 in PR (~7.5). At acidic pH, it has been difficult to observe an M-like state with a de-protonated Schiff base [52,122]. The direction of proton pumping was found to be inverted as seen by photocurrent measurements in reconstituted lipo-somes attached to BLM and in *Xenopus* oocytes under voltage-clamp conditions [52]. These findings were challenged by experiments reported by others [78,122] but have been confirmed in oocytes (Fig. 8B) [115], by fluorescence spectroscopy (Fig. 9) [87] and by cryo trapping experiments in the UV/vis [115] and in the IR [123], where the characteristic finger-print of an M-like intermediate was also observed at low pH values. These experiments confirm bidirectional proton transport in GPR as shown by Friedrich et al. [52]. The proton transport inverts in the physio-logical range around the pK_a of D97. The presented experimental approach offered a qualitative complementation to BLM measurements.

The reason for the change in vectoriality is thus a kinetic one: at acid-ic pH, the release of the SB proton towards the intracellular space is immediately followed by reprotonation, which can presumably occur from the water-filled cytoplasmic (CP) cavity and explains the lack of M-accumulation at room temperature. Although the mechanistic details of the inward H$^+$-transport mode of GPR are somewhat incomplete, it is evident, that an inwardly directed proton transport is only observed, if the proton acceptor position is neutralized by mutagenesis (GPR$_{D97N/T}$) or acidification [115]. Nevertheless, D97 might not act as a donor or ac-ceptor group under these conditions, and alternative residues for tran-sient de-/protonation still have to be identified.

One could also explain the current data with leakage, as pumping against the electrochemical gradient could not be demonstrated so far for experimental reasons. However, it was inferred from the different ap-plied light qualities (wavelength, intensity) that inward proton pumping requires a two photon cycle process, although green light alone is suffi-cient to induce inward currents (Figs. 8B, 9) [115]. A second light reaction akin to the above mentioned voltage dependence could help to accelerate proton transfer reactions as observed with blue light under acidic condi-tions. This could work in addition to the voltage effect and the high pK_a
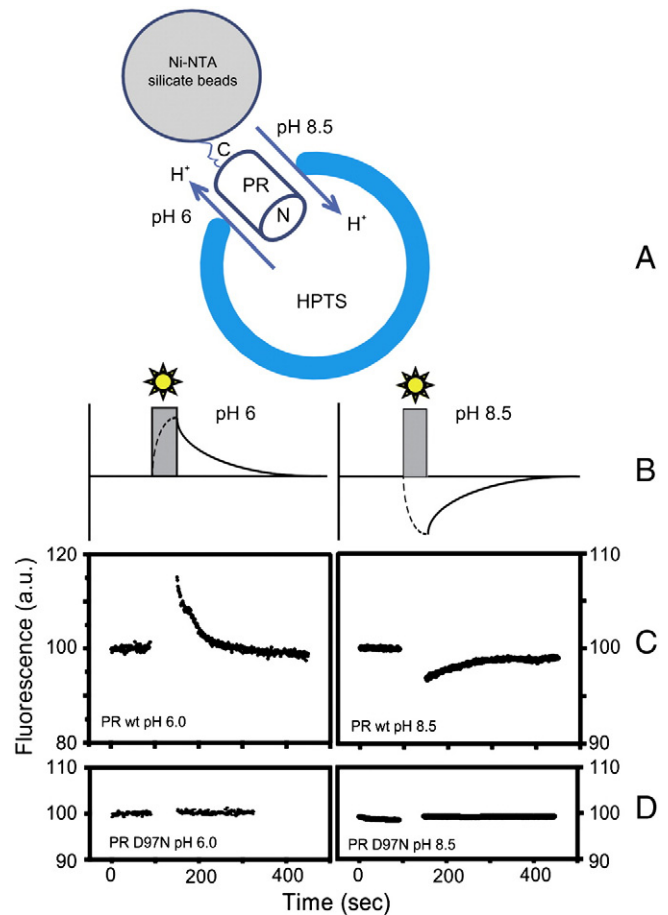
Fig. 9. Reversed proton transfer in GPR. C-terminally His-tagged PR was bound to Ni-NTA covered silicate beads, which enforced a unique orientation into proteoliposomes containing the pH-dependent fluorescent dye HPTS (A). Upon removal of the beads and sample illumi-nation, protons were either transferred out of the vesicles (pH 6, fluorescent increase) or to the inside (pH 8.5, fluorescence decrease) (B). Activity measurements of GPR and GPR$_{D97N}$ proteoliposomes at pH 6.0 and pH 8.5 reconstituted with Ni-NTA silicate beads (C). No fluo-rescent signal can be detected during the illumination period. GPR shows bidirectional trans-port, the net transport direction depending on the pH (fluorescence increase, proton export for pH 6; fluorescent decrease, proton import for pH 8.5). The D97N mutant shows no activ-ity over the whole pH range (constant fluorescence intensity) (D).
Figure taken from [87].

of D97. In the pR from *O. marina*, inward currents could not be detected in agreement with its low pK_a of the proton acceptor [40]. A two-photon photocycle is not uncommon in rhodopsins and has been ob-served before, for example in channelrhodopsins [124], but also in other retinylidene pumps like halorhodopsin [125,126]. In fact, a re-cently described tandem cassette allows fusion of two rhodopsin mole-cules and the determination of the relative pump transport activities [125]. This strategy could provide further insights into the voltage-dependence of pRs and their pumping efficiency under stationary con-ditions whose characterization become more relevant in the light of optogenetics.

5. Conclusions and outlook

Here, a survey of recent achievements in the proteorhodopsin field is presented stretching from initial characterizations of many different pRs to in-depth studies on the green absorbing variant (GPR). Noteworthy are the interactions of GPR with its environment. We have described sev-eral aspects covering the influence of the protein to photoisomerization, long ranging interactions within the molecule and the dynamics within the lipid bilayer. Some of the properties can be related to molecular and structural entities like the color coding residues or EF mobility

and photodynamics. Other topics remain open for further studies, such as the linkage between oligomerization state and function. Furthermore, the increasing number of pRs will provide new surprises and variations like they have been observed for the His-Asp cluster. And eventually there might be a linkage from the structure to the function to the phototrophic impact observed in the global phenomenon of proteorhodopsins. The presented studies also illustrate that advanced methodology such as dynamic nuclear polarization/solid-state NMR and time-resolved optical spectroscopy provides highly compatible data sets if properly combined and enables obtaining unprecedented insight into the molecular mechanism of retinal proteins.

Note added in proof

New high resolution structural data have been published during the finalization of the review. Atomic coordinates have been deposited in the protein data bank for BPRs from the γ-proteobacterium HOT75 (accession numbers 4KLY, 4KNF) and from an uncultured bacterium Med12 (4JQ6) [127]. A recent publication describes and discusses the structural properties of the pR from the *E. sibiricum* [128]. The latter one has further the novel property of using a lysine residue for the proton uptake pathway from the cytoplasmic side (D96 in bR) [129,130]. The structural aspects for the different pR molecules just emerge and will provide molecular details for the variations within the pR family that cannot be discussed here at the present stage. However, an initial comparison already reveals differences in important and above mentioned structural details. The BPRs come in a pentameric and hexameric state, while the pR from *E. sibiricum* only has a monomer as the biological unit. As discussed in [128], the orientation of the conserved histidine that is part of the His-Asp dyad is very different. In the *E. sibiricum* pR, the side chain is located within the monomeric unit pointing towards the conserved arginine that is part of the complex counter-ion. In contrast, the histidine in the BPR structures not only interacts with the proton acceptor aspartic residue (D85 in bR), but also protrudes into the space between the protomers. Here, it is hydrogen-bonded to the neighboring protomer by a tryptophane residue that is not conserved among the pRs. A comparison between the liquid-state NMR backbone structure of GPR (2L6XR) and the X-ray structure of BPR (4JQ6) shows similar secondary structure key features but also differences with respect to helix orientations. Reasons could be the very different sample conditions under which the liquid-state NMR data were acquired such as very high temperatures, different detergents and monomeric instead of pentameric/hexameric states. One should also bear in mind that the liquid-state NMR backbone structure has a relatively low resolution compared to the X-ray structure. The structural details obtained so far by many different methods will help our understanding in the functionality of pRs like the modulation of the His-Asp cluster, the presence of a PRG and the nature and importance of oligomeric states.

Acknowledgments

References

[1] C. Bamann, G. Nagel, E. Bamberg, Microbial rhodopsins in the spotlight, Curr. Opin. Neurobiol. 20 (2010) 610–616.

[2] G. Miesenböck, Optogenetic control of cells and circuits, Annu. Rev. Cell Dev. Biol. 27 (2011) 731–758.

[3] F. Zhang, J. Vierock, O. Yizhar, L.E. Fenno, S. Tsunoda, A. Kianianmomeni, M. Prigge, A. Berndt, J. Cushman, J. Polle, J. Magnuson, P. Hegemann, K. Deisseroth, The microbial opsin family of optogenetic tools, Cell 147 (2011) 1446–1457.

[4] O. Beja, L. Aravind, E.V. Koonin, M.T. Suzuki, A. Hadd, L.P. Nguyen, S.B. Jovanovich, C.M. Gates, R.A. Feldman, J.L. Spudich, E.N. Spudich, E.F. DeLong, Bacterial rhodopsin: evidence for a new type of phototrophy in the sea, Science 289 (2000) 1902–1906.

[5] K.W. Foster, J. Saranak, N. Patel, G. Zarilli, M. Okabe, T. Kline, K. Nakanishi, A rhodopsin is the functional photoreceptor for phototaxis in the unicellular eukaryote Chlamydomonas, Nature 311 (1984) 756–759.

[6] J.A. Bieszke, E.L. Braun, L.E. Bean, S. Kang, D.O. Natvig, K.A. Borkovich, The nop-1 gene of *Neurospora crassa* encodes a seven transmembrane helix retinal-binding protein homologous to archaeal rhodopsins, Proc. Natl. Acad. Sci. 96 (1999) 8034–8039.

[7] O.M. Finkel, O. Beja, S. Belkin, Global abundance of microbial rhodopsins, ISME J. 7 (2013) 448–451.

[8] J.L. Spudich, The multitalented microbial sensory rhodopsins, Trends Microbiol. 14 (2006) 480–487.

[9] J.L. Spudich, K.H. Jung, Microbial rhodopsins: phylogenetic and functional diversity, in: W.R. Briggs, J.L. Spudich (Eds.), Handbook of Photosensory Receptors, Wiley-VCH, Weinheim, 2005, pp. 1–24.

[10] E.F. DeLong, O. Béjà, The light-driven proton pump proteorhodopsin enhances bacterial survival during tough times, PLoS Biol. 8 (2010) e1000359.

[11] E.F. DeLong, The microbial ocean from genomes to biomes, Nature 459 (2009) 200–206.

[12] O. Beja, E.N. Spudich, J.L. Spudich, M. Leclerc, E.F. DeLong, Proteorhodopsin phototrophy in the ocean, Nature 411 (2001) 786–789.

[13] J.C. Venter, K. Remington, J.F. Heidelberg, A.L. Halpern, D. Rusch, J.A. Eisen, D. Wu, I. Paulsen, K.E. Nelson, W. Nelson, D.E. Fouts, S. Levy, A.H. Knap, M.W. Lomas, K. Nealson, O. White, J. Peterson, J. Hoffman, R. Parsons, H. Baden-Tillson, C. Pfannkoch, Y.-H. Rogers, H.O. Smith, Environmental genome shotgun sequencing of the Sargasso Sea, Science 304 (2004) 66–74.

[14] M.T. Cottrell, D.L. Kirchman, Photoheterotrophic microbes in the Arctic Ocean in summer and winter, Appl. Environ. Microbiol. 75 (2009) 4958–4966.

[15] J.R. de la Torre, L.M. Christianson, O. Béjà, M.T. Suzuki, D.M. Karl, J. Heidelberg, E.F. DeLong, Proteorhodopsin genes are distributed among divergent marine bacterial taxa, Proc. Natl. Acad. Sci. 100 (2003) 12830–12835.

[16] J. Frias-Lopez, Y. Shi, G.W. Tyson, M.L. Coleman, S.C. Schuster, S.W. Chisholm, E.F. DeLong, Microbial community gene expression in ocean surface waters, Proc. Natl. Acad. Sci. 105 (2008) 3805–3810.

[17] J. McCarren, E.F. DeLong, Proteorhodopsin photosystem gene clusters exhibit co-evolutionary trends and shared ancestry among diverse marine microbial phyla, Environ. Microbiol. 9 (2007) 846–858.

[18] G. Sabehi, R. Massana, J.P. Bielawski, M. Rosenberg, E.F. Delong, O. Béjà, Novel proteorhodopsin variants from the Mediterranean and Red Seas, Environ. Microbiol. 5 (2003) 842–849.

[19] S.J. Giovannoni, L. Bibbs, J.-C. Cho, M.D. Stapels, R. Desiderio, K.L. Vergin, M.S. Rappe, S. Laney, L.J. Wilhelm, H.J. Tripp, E.J. Mathur, D.F. Barofsky, Proteorhodopsin in the ubiquitous marine bacterium SAR11, Nature 438 (2005) 82–85.

[20] A.K. Sharma, O. Zhaxybayeva, R.T. Papke, W.F. Doolittle, Actinorhodopsins: proteorhodopsin-like gene sequences found predominantly in non-marine environments, Environ. Microbiol. 10 (2008) 1039–1056.

[21] M. Martinez-Garcia, B.K. Swan, N.J. Poulton, M.L. Gomez, D. Masland, M.E. Sieracki, R. Stepanauskas, High-throughput single-cell sequencing identifies photoheterotrophs and chemoautotrophs in freshwater bacterioplankton, ISME J. 6 (2012) 113–123.

[22] N. Atamna-Ismaeel, G. Sabehi, I. Sharon, K.-P. Witzel, M. Labrenz, K. Jurgens, T. Barkay, M. Stomp, J. Huisman, O. Beja, Widespread distribution of proteorhodopsins in freshwater and brackish ecosystems, ISME J. 2 (2008) 656–662.

[23] E.Y. Koh, N. Atamna-Ismaeel, A. Martin, R.O.M. Cowie, O. Beja, S.K. Davy, E.W. Maas, K.G. Ryan, Proteorhodopsin-bearing bacteria in Antarctic Sea ice, Appl. Environ. Microbiol. 76 (2010) 5918–5925.

[24] L.C. Bohorquez, C.A. Ruiz-Pérez, M.M. Zambrano, Proteorhodopsin-like genes present in thermoacidophilic high-mountain microbial communities, Appl. Environ. Microbiol. 78 (2012) 7813–7817.

[25] L.E. Petrovskaya, E.P. Lukashev, V.V. Chupin, S.V. Sychev, E.N. Lyukmanova, E.A. Kryukova, R.H. Ziganshin, E.V. Spirina, E.M. Rivkina, R.A. Khatypov, L.G. Erokhina, D.A. Gilichinsky, V.A. Shuvalov, M.P. Kirpichnikov, Predicted bacteriorhodopsin from *Exiguobacterium sibiricum* is a functional proton pump, FEBS Lett. 584 (2010) 4193–4196.

[26] N. Yutin, E. Koonin, Proteorhodopsin genes in giant viruses, Biol. Direct 7 (2012) 34.

[27] N.-U. Frigaard, A. Martinez, T.J. Mincer, E.F. DeLong, Proteorhodopsin lateral gene transfer between marine planktonic Bacteria and Archaea, Nature 439 (2006) 847–850.

[28] V. Iverson, R.M. Morris, C.D. Frazar, C.T. Berthiaume, R.L. Morales, E.V. Armbrust, Untangling genomes from metagenomes: revealing an uncultured class of marine euryarchaeota, Science 335 (2012) 587–590.

[29] O.K. Okamoto, J.W. Hastings, Novel dinoflagellate clock-related genes identified through microarray analysis, J. Phycol. 39 (2003) 519–526.

[30] C.H. Slamovits, N. Okamoto, L. Burri, E.R. James, P.J. Keeling, A bacterial proteorhodopsin proton pump in marine eukaryotes, Nat. Commun. 2 (2011) 183.

[31] A.J. Hartz, B.F. Sherr, E.B. Sherr, Photoresponse in the heterotrophic marine dinoflagellate *Oxyrrhis marina*, J. Eukaryot. Microbiol. 58 (2011) 171–177.

[32] J.A. Fuhrman, M.S. Schwalbach, U. Stingl, Proteorhodopsins: an array of physiological roles? Nat. Rev. Microbiol. 6 (2008) 488–494.

[33] A. Martinez, A.S. Bradley, J.R. Waldbauer, R.E. Summons, E.F. DeLong, Proteorhodopsin photosystem gene expression enables photophosphorylation in a heterologous host, Proc. Natl. Acad. Sci. 104 (2007) 5590–5595.

[34] J.M. Walter, D. Greenfield, C. Bustamante, J. Liphardt, Light-powering *Escherichia coli* with proteorhodopsin, Proc. Natl. Acad. Sci. 104 (2007) 2408–2412.

[35] L. Gomez-Consarnau, J.M. Gonzalez, M. Coll-Llado, P. Gourdon, T. Pascher, R. Neutze, C. Pedros-Alio, J. Pinhassi, Light stimulates growth of proteorhodopsin-containing marine Flavobacteria, Nature 445 (2007) 210–213.

[36] T. Riedel, L. Gómez-Consarnau, J. Tomasch, M. Martin, M. Jarek, J.M. González, S. Spring, M. Rohlfs, T. Brinkhoff, H. Cypionka, M. Göker, A. Fiebig, J. Klein, A. Goesmann, J.A. Fuhrman, I. Wagner-Döbler, Genomics and physiology of a marine flavobacterium

encoding a proteorhodopsin and a xanthorhodopsin-like protein, PLoS One 8 (2013) e57487.

[37] L. Gomez-Consarnau, N. Akram, K. Lindell, A. Pedersen, R. Neutze, D.L. Milton, J.M. Gonzalez, J. Pinhassi, Proteorhodopsin phototrophy promotes survival of marine bacteria during starvation, PLoS Biol. 8 (2010) e1000358.

[38] S.J. Giovannoni, U. Stingl, The importance of culturing bacterioplankton in the 'omics' age, Nat. Rev. Micro. 5 (2007) 820–826.

[39] Z. Wang, T.J. O'Shaughnessy, C.M. Soto, A.M. Rahbar, K.L. Robertson, N. Lebedev, G.J. Vora, Function and regulation of *Vibrio campbellii* Proteorhodopsin: acquired phototrophy in a classical organoheterotroph, PLoS One 7 (2012) e38749.

[40] C. Janke, F. Scholz, J. Becker-Baldus, C. Glaubitz, P.G. Wood, E. Bamberg, J. Wachtveitl, C. Bamann, Photocycle and vectorial proton transfer in a rhodopsin from the eukaryote *Oxyrrhis marina*, Biochemistry 52 (2013) 2750–2763.

[41] D. Man, W. Wang, G. Sabehi, L. Aravind, A.F. Post, R. Massana, E.N. Spudich, J.L. Spudich, O. Béjà, Diversification and spectral tuning in marine proteorhodopsins, EMBO J. 22 (2003) 1725–1731.

[42] S.P. Balashov, E.S. Imasheva, V.A. Boichenko, J. Anton, J.M. Wang, J.K. Lanyi, Xanthorhodopsin: a proton pump with a light-harvesting carotenoid antenna, Science 309 (2005) 2061–2064.

[43] T. Polivka, S.P. Balashov, P. Chabera, E.S. Imasheva, A. Yartsev, V. Sundstrom, J.K. Lanyi, Femtosecond carotenoid to retinal energy transfer in xanthorhodopsin, Biophys. J. 96 (2009) 2268–2277.

[44] S.P. Balashov, E.S. Imasheva, J.M. Wang, J.K. Lanyi, Excitation energy-transfer and the relative orientation of retinal and carotenoid in xanthorhodopsin, Biophys. J. 95 (2008) 2402–2414.

[45] H. Luecke, B. Schobert, J. Stagno, E.S. Imasheva, J.M. Wang, S.P. Balashov, J.K. Lanyi, Crystallographic structure of xanthorhodopsin, the light-driven proton pump with a dual chromophore, Proc. Natl. Acad. Sci. 105 (2008) 16561–16565.

[46] E.S. Imasheva, S.P. Balashov, A.R. Choi, K.-H. Jung, J.K. Lanyi, Reconstitution of *Gloeobacter violaceus* Rhodopsin with a light-harvesting carotenoid antenna, Biochemistry 48 (2009) 10948–10955.

[47] S.P. Balashov, E.S. Imasheva, A.R. Choi, K.-H. Jung, S.v. Liaaen-Jensen, J.K. Lanyi, Reconstitution of Gloeobacter Rhodopsin with Echinenone: role of the 4-keto group, Biochemistry 49 (2010) 9792–9799.

[48] F. Garczarek, K. Gerwert, Functional waters in intraprotein proton transfer monitored by FTIR difference spectroscopy, Nature 439 (2006) 109–112.

[49] S.P. Balashov, E.S. Imasheva, T.G. Ebrey, N. Chen, D.R. Menick, R.K. Crouch, Glutamate-194 to cysteine mutation inhibits fast light-induced proton release in bacteriorhodopsin, Biochemistry 36 (1997) 8671–8676.

[50] N. Pfleger, M. Lorch, A. Woerner, S. Shastri, C. Glaubitz, Characterisation of Schiff base and chromophore in green proteorhodopsin by solid-state NMR, J. Biomol. NMR 40 (2008) 15–21.

[51] A.K. Dioumaev, L.S. Brown, J. Shih, E.N. Spudich, J.L. Spudich, J.K. Lanyi, Proton transfers in the photochemical reaction cycle of proteorhodopsin, Biochemistry 41 (2002) 5348–5358.

[52] T. Friedrich, S. Geibel, R. Kalmbach, I. Chizhov, K. Ataka, J. Heberle, M. Engelhard, E. Bamberg, Proteorhodopsin is a light-driven proton pump with variable vectoriality, J. Mol. Biol. 321 (2002) 821–838.

[53] M. Mehler, F. Scholz, S.J. Ullrich, J. Mao, M. Braun, L.J. Brown, R.C.D. Brown, S.A. Fiedler, J. Becker-Baldus, J. Wachtveitl, C. Glaubitz, The EF loop in green proteorhodopsin affects conformation and photocycle dynamics, Biophys. J. 105 (2013) 385–396.

[54] L.C. Shi, M.A.M. Ahmed, W.R. Zhang, G. Whited, L.S. Brown, V. Ladizhansky, Three-dimensional solid-state NMR study of a seven-helical integral membrane proton pump-structural insights, J. Mol. Biol. 386 (2009) 1078–1093.

[55] L.C. Shi, E.M.R. Lake, M.A.M. Ahmed, L.S. Brown, V. Ladizhansky, Solid-state NMR study of proteorhodopsin in the lipid environment: secondary structure and dynamics, Biochim. Biophys. Acta (BBA) - Biomembr. 1788 (2009) 2563–2574.

[56] H. Luecke, B. Schobert, H.-T. Richter, J.-P. Cartailler, J.K. Lanyi, Structure of bacteriorhodopsin at 1.55 A resolution, J. Mol. Biol. 291 (1999) 899–911.

[57] S. Reckel, D. Gottstein, J. Stehle, F. Löhr, M.-K. Verhoefen, M. Takeda, R. Silvers, M. Kainosho, C. Glaubitz, J. Wachtveitl, F. Bernhard, H. Schwalbe, P. Güntert, V. Dötsch, Solution NMR structure of proteorhodopsin, Angew. Chem. Int. Ed. 50 (2011) 11942–11946.

[58] J. Yang, L. Aslimovska, C. Glaubitz, Molecular dynamics of proteorhodopsin in lipid bilayers by solid-state NMR, J. Am. Chem. Soc. 133 (2011) 4874–4881.

[59] F. Hempelmann, S. Hölper, M.-K. Verhoefen, A.C. Woerner, T. Köhler, S.-A. Fiedler, N. Pfleger, J. Wachtveitl, C. Glaubitz, His75-Asp97 cluster in green proteorhodopsin, J. Am. Chem. Soc. 133 (2011) 4645–4654.

[60] J. Stehle, F. Scholz, F. Lohr, S. Reckel, C. Roos, M. Blum, M. Braun, C. Glaubitz, V. Dötsch, J. Wachtveitl, H. Schwalbe, Characterization of the ground state dynamics of proteorhodopsin by NMR and optical spectroscopies, J. Biomol. NMR 54 (2012) 401–413.

[61] R. Partha, R. Krebs, T.L. Caterino, M.S. Braiman, Weakened coupling of conserved arginine to the proteorhodopsin chromophore and its counterion implies structural differences from bacteriorhodopsin, Biochim. Biophys. Acta Bioenerg. 1708 (2005) 6–12.

[62] S. Shastri, J. Vonck, N. Pfleger, W. Haase, W. Kuehlbrandt, C. Glaubitz, Proteorhodopsin: characterisation of 2D crystals by electron microscopy and solid state NMR, Biochim. Biophys. Acta 1768 (2007) 3012–3019.

[63] A.L. Klyszejko, S. Shastri, S.A. Mari, H. Grubmuller, D.J. Muller, C. Glaubitz, Folding and assembly of proteorhodopsin, J. Mol. Biol. 376 (2008) 35–41.

[64] J. Hoffmann, L. Aslimovska, C. Bamann, C. Glaubitz, E. Bamberg, B. Brutschy, Studying the stoichiometries of membrane proteins by mass spectrometry: microbial rhodopsins and a potassium ion channel, Phys. Chem. Chem. Phys. 12 (2010) 3480.

[65] K.M. Stone, J. Voska, M. Kinnebrew, A. Pavlova, M.J.N. Junk, S.G. Han, Structural insight into proteorhodopsin oligomers, Biophys. J. 104 (2013) 472–481.

[66] R. Krebs, U. Alexiev, R. Partha, A. DeVita, M. Braiman, Detection of fast light-activated H+ release and M intermediate formation from proteorhodopsin, BMC Physiol. 2 (2002) 5.

[67] J.M. Kralj, E.N. Spudich, J.L. Spudich, K.J. Rothschild, Raman spectroscopy reveals direct chromophore interactions in the Leu/Gln105 spectral tuning switch of proteorhodopsins, J. Phys. Chem. B 112 (2008) 11770–11776.

[68] S.P. Balashov, L.E. Petrovskaya, E.P. Lukashev, E.S. Imasheva, A.K. Dioumaev, J.M. Wang, S.V. Sychev, D.A. Dolgikh, A.B. Rubin, M.P. Kirpichnikov, J.K. Lanyi, Aspartate–histidine interaction in the retinal Schiff base counterion of the light-driven proton pump of *Exiguobacterium sibiricum*, Biochemistry 51 (2012) 5748–5762.

[69] T. Tsukamoto, T. Kikukawa, T. Kurata, K.-H. Jung, N. Kamo, M. Demura, Salt bridge in the conserved His–Asp cluster in Gloeobacter rhodopsin contributes to trimer formation, FEBS Lett. 587 (2013) 322–327.

[70] M.J. Ranaghan, C.T. Schwall, N.N. Alder, R.R. Birge, Green proteorhodopsin reconstituted into nanoscale phospholipid bilayers (nanodiscs) as photoactive monomers, J. Am. Chem. Soc. 133 (2011) 18318–18327.

[71] K. Mörs, C. Roos, F. Scholz, J. Wachtveitl, V. Dötsch, F. Bernhard, C. Glaubitz, Modified lipid and protein dynamics in nanodiscs, Biochim. Biophys. Acta 1828 (2013) 1222–1229.

[72] W.-W. Wang, O.A. Sineshchekov, E.N. Spudich, J.L. Spudich, Spectroscopic and photochemical characterization of a deep ocean proteorhodopsin, J. Biol. Chem. 278 (2003) 33985–33991.

[73] M. Yoshitsugu, M. Shibata, D. Ikeda, Y. Furutani, H. Kandori, Color change of proteorhodopsin by a single amino acid replacement at a distant cytoplasmic loop, Angew. Chem. Int. Ed. 47 (2008) 3923–3926.

[74] M. Yoshitsugu, J. Yamada, H. Kandori, Color-changing mutation in the E–F loop of proteorhodopsin, Biochemistry 48 (2009) 4324–4330.

[75] J. Otomo, Influence exercised by histidine-95 on chloride transport and the photocycle in halorhodopsin, Biochemistry 35 (1996) 6684–6689.

[76] K. Yamada, A. Kawanabe, H. Kandori, Importance of alanine at position 178 in proteorhodopsin for absorption of prevalent ambient light in the marine environment, Biochemistry 49 (2010) 2416–2423.

[77] G. Varo, L.S. Brown, M. Lakatos, J.K. Lanyi, Characterization of the photochemical reaction cycle of proteorhodopsin, Biophys. J. 84 (2003) 1202–1207.

[78] M. Lakatos, J.K. Lanyi, J. Szakács, G. Váró, The photochemical reaction cycle of proteorhodopsin at low pH, Biophys. J. 84 (2003) 3252–3256.

[79] S. Subramaniam, R. Henderson, Molecular mechanism of vectorial proton translocation by bacteriorhodopsin, Nature 406 (2000) 653–657.

[80] J.K. Lanyi, H. Luecke, Bacteriorhodopsin, Curr. Opin. Struct. Biol. 11 (2001) 415–419.

[81] T. Hirai, S. Subramaniam, Protein conformational changes in the bacteriorhodopsin photocycle: comparison of findings from electron and X-ray crystallographic analyses, PLoS One 4 (2009) e5769.

[82] J. Vonck, Structure of the bacteriorhodopsin mutant F219L N intermediate revealed by electron crystallography, EMBO J. 19 (2000) 2152–2160.

[83] T.E. Thorgeirsson, W.Z. Xiao, L.S. Brown, R. Needleman, J.K. Lanyi, Y.K. Shin, Transient channel-opening in bacteriorhodopsin: an EPR study, J. Mol. Biol. 273 (1997) 951–957.

[84] S. Hussain, J.M. Franck, S. Han, Transmembrane protein activation refined by site-specific hydration dynamics, Angew. Chem. Int. Ed. 52 (2013) 1953–1958.

[85] R. Rangarajan, J.F. Galan, G. Whited, R.R. Birge, Mechanism of spectral tuning in green-absorbing proteorhodopsin, Biochemistry 46 (2007) 12679–12686.

[86] V.B. Bergo, O.A. Sineshchekov, J.M. Kralj, R. Partha, E.N. Spudich, K.J. Rothschild, J.L. Spudich, His-75 in proteorhodopsin, a novel component in light-driven proton translocation by primary pumps, J. Biol. Chem. 284 (2009) 2836–2843.

[87] N. Pfleger, A.C. Wörner, J. Yang, S. Shastri, U.A. Hellmich, L. Aslimovska, M.S.M. Maier, C. Glaubitz, Solid-state NMR and functional studies on proteorhodopsin, Biochim. Biophys. Acta Bioenerg. 1787 (2009) 697–705.

[88] L.F. Pacios, O. Gálvez, Variation of atomic charges on proton transfer in strong hydrogen bonds: the case of anionic and neutral imidazole-acetate complexes, J. Comput. Chem. 27 (2006) 1650–1661.

[89] R. Huber, T. Kohler, M.O. Lenz, E. Bamberg, R. Kalmbach, M. Engelhard, J. Wachtveitl, pH-dependent photoisomerization of retinal in proteorhodopsin, Biochemistry 44 (2005) 1800–1806.

[90] M.O. Lenz, R. Huber, B. Schmidt, P. Gilch, R. Kalmbach, M. Engelhard, J. Wachtveitl, First steps of retinal photoisomerization in proteorhodopsin, Biophys. J. 91 (2006) 255–262.

[91] K. Neumann, M.-K. Verhoefen, I. Weber, C. Glaubitz, J. Wachtveitl, Initial reaction dynamics of proteorhodopsin observed by femtosecond infrared and visible spectroscopy, Biophys. J. 94 (2008) 4796–4807.

[92] M.-K. Verhoefen, K. Neumann, I. Weber, C. Glaubitz, J. Wachtveitl, Primary reaction dynamics of proteorhodopsin mutant D97N observed by femtosecond infrared and visible spectroscopy†, Photochem. Photobiol. 85 (2009) 540–546.

[93] M.O. Lenz, A.C. Woerner, C. Glaubitz, J. Wachtveitl, Photoisomerization in proteorhodopsin mutant D97N, Photochem. Photobiol. 83 (2007) 226–231.

[94] J. Herz, M.-K. Verhoefen, I. Weber, C. Bamann, C. Glaubitz, J. Wachtveitl, Critical role of Asp227 in the photocycle of proteorhodopsin, Biochemistry 51 (2012) 5589–5600.

[95] M. Andersson, E. Malmerberg, S. Westenhoff, G. Katona, M. Cammarata, A.B. Wöhri, L.C. Johansson, F. Ewald, M. Eklund, M. Wulff, J. Davidsson, R. Neutze, Structural dynamics of light-driven proton pumps, Structure 17 (2009) 1265–1275.

[96] J. Heberle, Proton transfer reactions across bacteriorhodopsin and along the membrane, Biochim. Biophys. Acta Bioenerg. 1458 (2000) 135–147.

[97] L. Keszthelyi, P. Ormos, Displacement current on purple membrane fragments oriented in a suspension, Biophys. Chem. 18 (1983) 397–405.

[98] T.R. Herrmann, G.W. Rayfield, The electrical response to light of bacteriorhodopsin in planar membranes, Biophys. J. 21 (1978) 111–125.

[99] H.W. Trissl, M. Montal, Electrical demonstration of rapid light-induced conformational changes in bacteriorhodopsin, Nature 266 (1977) 655–657.

[100] L.A. Drachev, V.N. Frolov, A.D. Kaulen, E.A. Liberman, S.A. Ostroumov, V.G. Plakunova, A.Y. Semenov, V.P. Skulachev, Reconstitution of biological molecular generators of electric current. Bacteriorhodopsin, J. Biol. Chem. 251 (1976) 7059–7065.

[101] A. Der, P. Hargittai, J. Simon, Time-resolved photoelectric and absorption signals from oriented purple membranes immobilized in gel, J. Biochem. Biophys. Methods 10 (1985) 295–300.

[102] C.F. Fowler, B. Kok, Direct observation of a light-induced electric field in chloroplasts, Biochim. Biophys. Acta Bioenerg. 357 (1974) 308–318.

[103] O.A. Sineshchekov, J.L. Spudich, Light-induced intramolecular charge movements in microbial rhodopsins in intact *E. coli* cells, Photochem. Photobiol. Sci. 3 (2004) 548–554.

[104] O.A. Sineshchekov, K.-H. Jung, J.L. Spudich, From the cover: two rhodopsins mediate phototaxis to low- and high-intensity light in *Chlamydomonas reinhardtii*, PNAS 99 (2002) 8689–8694.

[105] M. Holz, M. Lindau, M.P. Heyn, Distributed kinetics of the charge movements in bacteriorhodopsin: evidence for conformational substates, Biophys. J. 53 (1988) 623–633.

[106] T.A. Krulwich, G. Sachs, E. Padan, Molecular aspects of bacterial pH sensing and homeostasis, Nat. Rev. Microbiol. 9 (2011) 330–343.

[107] G. Nagel, B. Mockel, G. Buldt, E. Bamberg, Functional expression of bacteriorhodopsin in oocytes allows direct measurement of voltage dependence of light induced H+ pumping, FEBS Lett. 377 (1995) 263–266.

[108] S.P. Tsunoda, D. Ewers, S. Gazzarrini, A. Moroni, D. Gradmann, P. Hegemann, H+-pumping rhodopsin from the marine alga Acetabularia, Biophys. J. 91 (2006) 1471–1479, http://dx.doi.org/10.1529/biophysj.106.086421.

[109] A. Seki, S. Miyauchi, S. Hayashi, T. Kikukawa, M. Kubo, M. Demura, V. Ganapathy, N. Kamo, Heterologous expression of pharaonis halorhodopsin in *Xenopus laevis* oocytes and electrophysiological characterization of its light-driven C-pump activity, Biophys. J. 92 (2007) 2559–2569.

[110] L.S. Brown, J. Sasaki, H. Kandori, A. Maeda, R. Needleman, J.K. Lanyi, Glutamic acid 204 is the terminal proton release group at the extracellular surface of bacteriorhodopsin, J. Biol. Chem. 270 (1995) 27122–27126.

[111] M.R.M. Miranda, A.R. Choi, L. Shi, A.G. Bezerra Jr., K.-H. Jung, L.S. Brown, The photocycle and proton translocation pathway in a cyanobacterial ion-pumping rhodopsin, Biophys. J. 96 (2009) 1471–1481.

[112] Y. Xiao, R. Partha, R. Krebs, M. Braiman, Time-resolved FTIR spectroscopy of the photointermediates involved in fast transient H+ release by proteorhodopsin, J. Phys. Chem. B 109 (2004) 634–641.

[113] V.A. Lórenz-Fonfría, T. Resler, N. Krause, M. Nack, M. Gossing, G. Fischer von Mollard, C. Bamann, E. Bamberg, R. Schlesinger, J. Heberle, Transient protonation changes in channelrhodopsin-2 and their relevance to channel gating, Proc. Natl. Acad. Sci. U.S.A. 110 (2013) E1273–E1281.

[114] M. Nack, I. Radu, B.-J. Schultz, T. Resler, R. Schlesinger, A.-N. Bondar, C. del Val, S. Abbruzzetti, C. Viappiani, C. Bamann, E. Bamberg, J. Heberle, Kinetics of proton release and uptake by channelrhodopsin-2, FEBS Lett. 586 (2012) 1344–1348.

[115] É. Lörinczi, M.-K. Verhoefen, J. Wachtveitl, A.C. Woerner, C. Glaubitz, M. Engelhard, E. Bamberg, T. Friedrich, Voltage- and pH-dependent changes in vectoriality of photocurrents mediated by wild-type and mutant proteorhodopsins upon expression in Xenopus oocytes, J. Mol. Biol. 393 (2009) 320–341.

[116] S. Moltke, M.P. Heyn, Photovoltage kinetics of the acid-blue and acid-purple forms of bacteriorhodopsin: evidence for no net charge transfer, Biophys. J. 69 (1995) 2066–2073.

[117] X. Jiang, M. Engelhard, K. Ataka, J. Heberle, Molecular impact of the membrane potential on the regulatory mechanism of proton transfer in sensory rhodopsin II, J. Am. Chem. Soc. 132 (2010) 10808–10815.

[118] X. Jiang, E. Zaitseva, M. Schmidt, F. Siebert, M. Engelhard, R. Schlesinger, K. Ataka, R. Vogel, J. Heberle, Resolving voltage-dependent structural changes of a membrane photoreceptor by surface-enhanced IR difference spectroscopy, Proc. Natl. Acad. Sci. 105 (2008) 12113–12117.

[119] J. Holterhues, E. Bordignon, D. Klose, C. Rickert, Johann P. Klare, S. Martell, L. Li, M. Engelhard, H.-J. Steinhoff, The signal transfer from the receptor NpSRII to the transducer NpHtrII is not hampered by the D75N mutation, Biophys. J. 100 (2011) 2275–2282.

[120] G. Nagel, B. Kelety, B. Mockel, G. Buldt, E. Bamberg, Voltage dependence of proton pumping by bacteriorhodopsin is regulated by the voltage-sensitive ratio of M1 to M2, Biophys. J. 74 (1998) 403–412.

[121] S. Geibel, T. Friedrich, P. Ormos, P.G. Wood, G. Nagel, E. Bamberg, The voltage-dependent proton pumping in bacteriorhodopsin is characterized by optoelectric behavior, Biophys. J. 81 (2001) 2059–2068.

[122] A.K. Dioumaev, J.M. Wang, Z. Bálint, G. Váró, J.K. Lanyi, Proton transport by proteorhodopsin requires that the retinal Schiff base counterion Asp-97 Be anionic, Biochemistry 42 (2003) 6582–6587.

[123] M.K. Verhoefen, G. Schafer, S. Shastri, I. Weber, C. Glaubitz, W. Mantele, J. Wachtveitl, Low temperature FTIR spectroscopy provides new insights in the pH-dependent proton pathway of proteorhodopsin, Biochim. Biophys. Acta 1807 (2011) 1583–1590.

[124] G. Nagel, T. Szellas, W. Huhn, S. Kateriya, N. Adeishvili, P. Berthold, D. Ollig, P. Hegemann, E. Bamberg, Channelrhodopsin-2, a directly light-gated cation-selective membrane channel, Proc. Natl. Acad. Sci. U.S.A. 100 (2003) 13940–13945.

[125] S. Kleinlogel, U. Terpitz, B. Legrum, D. Gokbuget, E.S. Boyden, C. Bamann, P.G. Wood, E. Bamberg, A gene-fusion strategy for stoichiometric and co-localized expression of light-gated membrane proteins, Nat. Methods 8 (2011) 1083–1088.

[126] P. Hegemann, D. Oesterhelt, E. Bamberg, The transport activity of the light-driven chloride pump halorhodopsin is regulated by green and blue light, Biochim. Biophys. Acta (BBA) - Biomembr. 819 (1985) 195–205.

[127] T. Ran, G. Ozorowski, Y. Gao, O.A. Sineshchekov, W. Wang, J.L. Spudich, H. Luecke, Cross-protomer interaction with the photoactive site in oligomeric proteorhodopsin complexes, Acta Crystallographica Section D 69 (2013) 1965–1980.

[128] I. Gushchin, P. Chervakov, P. Kuzmichev, A.N. Popov, E. Round, V. Borshchevskiy, A. Ishchenko, L. Petrovskaya, V. Chupin, D.A. Dolgikh, A.S. Arseniev, M. Kirpichnikov, V. Gordeliy, Structural insights into the proton pumping by unusual proteorhodopsin from nonmarine bacteria, Proc. Natl. Acad. Sci. 110 (2013) 12631–12636.

[129] A.K. Dioumaev, L.E. Petrovskaya, J.M. Wang, S.P. Balashov, D.A. Dolgikh, M.P. Kirpichnikov, J.K. Lanyi, Photocycle of *Exiguobacterium sibiricum* rhodopsin characterized by Low-temperature trapping in the IR and time-resolved studies in the visible, J. Phys. Chem. B 117 (2013) 7235–7253.

[130] S.P. Balashov, L.E. Petrovskaya, E.S. Imasheva, E.P. Lukashev, A.K. Dioumaev, J.M. Wang, S.V. Sychev, D.A. Dolgikh, A.B. Rubin, M.P. Kirpichnikov, J.K. Lanyi, Breaking the carboxyl rule: lysine 96 facilitates reprotonation of the Schiff base in the photocycle of a retinal protein from *Exiguobacterium sibiricum*, J. Biol. Chem. 288 (2013) 21254–21265.